Local hydrated structure of an Fe^{2+}/Fe^{3+} aqueous solution: an investigation using a combination of molecular dynamics and X-ray absorption fine structure methods*

YE Qing(叶青)[1] CHEN Xing(陈兴)[2,1)] ZHOU Jing(周靖)[1] ZHAO Hai-Feng(赵海峰)[1]
CHU Wang-Sheng(储旺盛)[2] ZHENG Xu-Sheng(郑旭升)[2] Augusto. Marcelli[3,2)]
WU Zi-Yu(吴自玉)[1,2,3)]

[1] Beijing Synchrotron Radiation Facility, Institute of High Energy Physics, Chinese Academy of Sciences, Beijing 100049, China
[2] National Synchrotron Radiation Laboratory, University of Science and Technology of China, Hefei 230029, China
[3] Istituto Nazionale di Fisica Nucleare, Laboratori Nazionali di Frascati, Frascati 00044, Italy

Abstract: The hydrated shell of both Fe^{2+} and Fe^{3+} aqueous solutions are investigated by using the molecular dynamics (MD) and X-ray absorption structure (XAS) methods. The MD simulations show that the first hydrated shells of both Fe^{2+} and Fe^{3+} are characterized by a regular octahedron with an Fe-O distance of 2.08Å for Fe^{2+} and 1.96Å for Fe^{3+}, and rule out the occurrence of a Jahn-Teller distortion in the hydrated shell of an Fe^{2+} aqueous solution. The corresponding X-ray absorption near edge fine structure (XANES) calculation successfully reproduces all features in the XANES spectra in Fe^{2+} and Fe^{3+} aqueous solution. A feature that is located at energy 1 eV higher than the white line (WL) in an Fe^{3+} aqueous solution may be assigned to the contribution of the charge transfer.

Key words: Fe^{2+} and Fe^{3+}, aqueous solution, XAS, molecular dynamics

PACS: 61.05.-a, 61.05.cj, 61.20.Ja **DOI:** 10.1088/1674-1137/37/3/038003

1 Introduction

Metal cation aqueous solutions are involved in many chemical processes and play an important role. For instance, the formation and extraction of minerals [1, 2], stabilization of surfaces and nanoparticles [3, 4], solvated ion activating biochemical reactions [5, 6], as well as transport mechanisms of toxic elements [7]. All these processes involve the interaction between hydrated cations and coordinated species, which has an impact on the polarization extent of hydrated waters, hydrogen bonding of water molecules in hydrated shells, and the formation of cation pairs. It is fundamental to identify the geometrical structures and dynamic properties of hydrated shells in cation aqueous solution in order to understand and describe the different mechanisms in all chemical processes.

Many investigations have been carried out to identify the local hydrated structure of both Fe^{2+} and Fe^{3+} aqueous solutions and conflicts exist among these works. In the early 90s, Floris et al. pointed out that Fe^{2+} and Fe^{3+} aqueous solutions were characterized by a regular octahedron in the first hydrated shell by using classical MD simulation [8]. Tawun and Bernd gave a 2.10Å Fe-O distance for Fe^{2+} and 2.02Å for Fe^{3+} by using a more accurate QM/MM simulation [9]. In 2004, Jarzecki et al. considered the influence of bulk water and found that an $Fe^{2+}(H_2O)_6$ cluster was characterized by a Jahn-Teller distortion with a different Fe-O distance [10–12]. However, all the work mentioned above involves theoretical calculations only, there is no experimental evidence. A combination of the theoretical result with experimental data will be better for achieving a detailed understanding and description of the hydrated structure of Fe^{2+}/Fe^{3+} aqueous solutions

The structure of an aqueous solution surrounding an individual ion is difficult to detect directly, therefore, the combination of MD and XAS will be a good method for the detection of the structure of a metal ion in aqueous solution. In this paper, we will give a reliable hydrated

Received 27 April 2012, Revised 14 August 2012

* Supported by Knowledge Innovation Program of the Chinese Academy of Sciences (KJCX2-YW-N42), Key Important Project of National Natural Science Foundation of China (10734070), National Natural Science Foundation of China (NSFC 11079031, 10805055, 10905067) and National Basic Research Program of China (2009CB930804)

1) E-mail: chenxing@ustc.edu.cn

2) E-mail: marcelli@lnf.infn.it

3) E-mail: wuzy@ustc.edu.cn

structure for Fe^{2+}/Fe^{3+} aqueous solutions by using a combination of MD and XAS investigations. The investigation points out that Fe^{2+}/Fe^{3+} aqueous solutions are both characterized by a regular octahedron and the distances of the Fe-O bond in the first hydrated shell are 2.08Å and 1.96Å for Fe^{2+} and Fe^{3+}, respectively. No Jahn-Teller distortion has been observed in the Fe^{2+} aqueous solution. A feature that locates at energy 1 eV higher than the white line (WL) in Fe^{3+} aqueous solution may be assigned to the contribution of the charge transfer.

2 Theoretical calculation and experiments

2.1 Force field and scheme of molecular dynamics

In order to obtain enough reliable sample space to reproduce the X-ray absorption spectra, we have to simulate a long thermal motion in both Fe^{2+}/Fe^{3+} aqueous solutions (∼ns level). To obtain the force field to describe the interaction between Fe^{2+}/Fe^{3+}-water molecules, the first principle method is used to scan the potential energy surface (PES) of Fe^{2+}/Fe^{3+}-H_2O. The PES has been fitted with an empirical potential, which has been employed to describe the interaction between a cation and H_2O during MD simulations.

We employed the restricted open shell Hartree-Fock theory [13] with a Lanl2dz valence electron basis and the corresponding core pseudo-potential to describe Fe [14, 15], cc-PVTZ basis to O and H atoms [16, 17]. The PCM model is used to consider the bulk water effect, the cavity radii in the PCM model is optimized and given 1.072Å for Fe^{2+}, 1.022Å for Fe^{3+}, 1.68Å for oxygen and 1.44Å for hydrogen based on the previously described method, which enables our calculated pair Fe^{2+}/Fe^{3+}-water molecule potential to contain the contribution of the three-body term [18]. The SPC/E model is employed to describe the water molecule.

The scanned PES of the Fe^{3+}-H_2O and Fe^{2+}-H_2O is fitted by using Eqs. (1) and (2), respectively.

$$\begin{aligned} U_{\text{Fe-water}} = {} & \frac{q_{\text{Fe}}q_{\text{O}}}{\varepsilon r_{\text{Fe-O}}}+\frac{A_{\text{O}}}{r^4_{\text{Fe-O}}}+\frac{B_{\text{O}}}{r^6_{\text{Fe-O}}}+\frac{C_{\text{O}}}{r^8_{\text{Fe-O}}}+\frac{D_{\text{O}}}{r^{12}_{\text{Fe-O}}} \\ & +E_{\text{O}}\exp(-F_{\text{O}}r_{\text{Fe-O}})+\frac{q_{\text{Fe}}q_{\text{H}}}{\varepsilon r_{\text{Fe-H}}}+\frac{A_{\text{H}}}{r^4_{\text{Fe-H}}} \\ & +\frac{B_{\text{H}}}{r^6_{\text{Fe-H}}}+\frac{C_{\text{H}}}{r^8_{\text{Fe-H}}}+\frac{D_{\text{H}}}{r^{12}_{\text{Fe-H}}}, \end{aligned} \tag{1}$$

$$\begin{aligned} U_{\text{Fe-water}} = {} & \frac{q_{\text{Fe}}q_{\text{O}}}{\varepsilon r_{\text{Fe-O}}}-\frac{C}{r^4_{\text{Fe-O}}}-\frac{D}{r^6_{\text{Fe-O}}}-\frac{F}{r^{12}_{\text{Fe-O}}} \\ & +A\exp(-Br_{\text{Fe-O}})+\frac{q_{\text{Fe}}q_{\text{H}}}{\varepsilon r_{\text{Fe-H}_1}}+\frac{q_{\text{Fe}}q_{\text{H}}}{\varepsilon r_{\text{Fe-H}_2}}, \end{aligned} \tag{2}$$

where q_{Fe} refers to the charge of Fe^{n+} cation (n=2 or 3), and q_{O} and q_{H} are the charges centered at the oxygen and hydrogen site in the water molecule. Here we use the values defined by the SPC/E model, −0.8476 a.u. for an oxygen atom and 0.4238 a.u. for a hydrogen atom. $r_{\text{Fe-O}}$ and $r_{\text{Fe-H}}$ are the distances of Fe-O and Fe-H, respectively, A_{O}, B_{O}, C_{O}, D_{O}, E_{O}, F_{O}, A_{H}, B_{H}, C_{H}, D_{H}, A, B, C and D are the fit parameters. The fit is carried out by a combination of the quasi Newton method and the universal global optimization (UGO) algorithm; the corresponding fit parameters are shown in Table 1.

The interaction model between Fe^{2+}/Fe^{3+} cations and water molecules, e.g., Eqs. (1) and (2), have been embedded in a modified GROMACS package to carry out the MD simulation [19]. In the MD simulation, one Fe^{2+}/Fe^{3+} cation and 507 water molecules were confined in a 25Å×25Å×25Å box with a periodic boundary condition. A cut-off of 10 Å was used to deal with the nonbonded interaction as well as the electrostatic interaction. The particle mesh Ewald method [20] was used to take care of the long-range electrostatic effects. A homogeneous background charge was used to compensate for the presence of the Fe^{2+}/Fe^{3+} cation. The simulations were carried out in the NVT ensemble, coupled with a Berendsen heating bath at a coupling constant of 0.1 ps [21]. The simulation lasts for 105 ns with steps of one fs, while the actual configuration has been stored every 0.5 ps.

Table 1. The best-fit parameters of the Fe^{2+}/Fe^{3+} cation-water effective pair potential.

Fe^{3+}	$A_{\text{O}}/(\text{kJ}\cdot\text{mol}^{-1}\cdot\text{nm}^4)$	$B_{\text{O}}/(\text{kJ}\cdot\text{mol}^{-1}\cdot\text{nm}^6)$	$C_{\text{O}}/(\text{kJ}\cdot\text{mol}^{-1}\cdot\text{nm}^8)$	$D_{\text{O}}/(\text{kJ}\cdot\text{mol}^{-1}\cdot\text{nm}^{12})$	$E_{\text{O}}/(\text{kJ}\cdot\text{mol}^{-1})$
	−0.07468	0.09285	−0.00147	1.14255×10^{-7}	−70759.14122
	$F_{\text{O}}/(\text{nm}^{-1})$	$A_{\text{H}}/(\text{kJ}\cdot\text{mol}^{-1}\cdot\text{nm}^4)$	$B_{\text{H}}/(\text{kJ}\cdot\text{mol}^{-1}\cdot\text{nm}^6)$	$C_{\text{H}}/(\text{kJ}\cdot\text{mol}^{-1}\cdot\text{nm}^8)$	$D_{\text{H}}/(\text{kJ}\cdot\text{mol}^{-1}\cdot\text{nm}^{12})$
	22.18280	−0.14551	0.00347	-1.86834×10^{-5}	1.66963×10^{-10}
Fe^{2+}	$A/(\text{kJ}\cdot\text{mol}^{-1})$	B/nm^{-1}	$C/(\text{kJ}\cdot\text{mol}^{-1}\cdot\text{nm}^4)$	$D/(\text{kJ}\cdot\text{mol}^{-1}\cdot\text{nm}^6)$	$F/(\text{kJ}\cdot\text{mol}^{-1}\cdot\text{nm}^{12})$
	3478.966	11.52	1.21880	-3.03884×10^{-2}	3.17817×10^{-8}

2.2 The XAS experiment and XANES calculation

The XAS experiment: analytical grade $FeCl_2$ and $FeCl_3$ are used for 0.1M Fe^{2+}/Fe^{3+} aqueous solution. The Fe-K edge XAS spectra of the fresh Fe^{2+}/Fe^{3+} aqueous solution were collected at the XAFS station of the Beijing Synchrotron Radiation Facility (BSRF) with the storage ring working at 2.2 GeV with an average electron current of 80 mA. The X-ray beam was monochromatized by a double-crystal Si(111) monochromator characterized at the energy resolution $\Delta E/E \sim 3\times10^{-4}$. Solutions were measured with a Teflon cell and the thickness of the solution was adjusted by optimizing the absorption thickness $\Delta\mu d \approx 1$. $\Delta\mu$ is the absorption edge jump and d is the thickness of the solution inside the cell. The XAS spectra at the Au-L_3 edge were recorded in transmission mode at room temperature and both incident and transmission intensities were detected using two ionization chambers placed before and after the liquid cell.

The XANES calculation: the XANES calculations, based on a self-consistent multiple-scattering (MS) method, were carried out using the FEFF8.2 code [22]. We chose the Hedin-Lundqvist (H-L) model for the exchange correlation part of the potential. The spectra were first background subtracted by fitting the pre-edge using a least-square method and then all spectra were normalized to one at energies far from the edge.

3 Results and discussion

3.1 The hydrated shell configuration

Figure 1 shows the radial distribution function of the Fe^{2+} and Fe^{3+} aqueous solution and the corresponding running integration number. It can be seen that Fe^{2+} and Fe^{3+} aqueous solution have a very concentrated first hydrated shell and the first peak of Fe^{3+}-O $g(r)$ locates at 1.96Å while Fe^{2+}-O $g(r)$ locates at 2.08Å. For Fe^{3+} aqueous solution, the second hydrated shell ranges between 3.5Å and 4.72Å while Fe^{2+} aqueous solution ranges from 3.8Å to 5.02Å. An apparent separation between the first and second hydrated shell was observed in both Fe^{2+} and Fe^{3+} aqueous solutions, indicating that water exchange process between the first and second shell are rare. The first hydrated shell coordination number of both Fe^{2+} and Fe^{3+} aqueous solution is 6, pointing out a relatively weak structural disorder contribution. At the same time, the first peak in the Fe^{3+}-O $g(r)$ is relatively more intense than its Fe^{2+}-O $g(r)$ counterpart, which implies that the hydrated structure of the Fe^{3+} aqueous solution is relatively more stable than the Fe^{2+} aqueous solution. We attribute the difference to a strong constrain effect due to the relatively high positive charge of an Fe^{3+} cation.

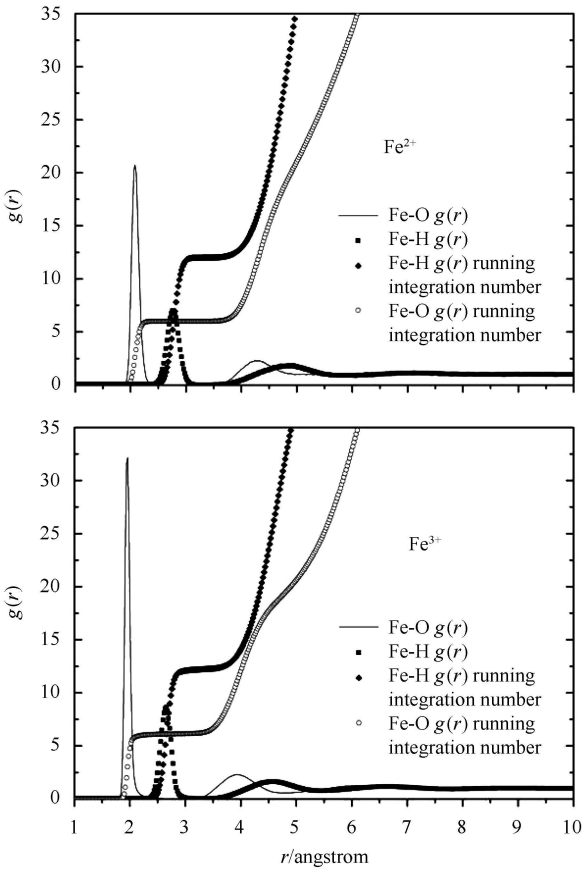

Fig. 1. The radial distribution functions and corresponding running integrate numbers of both Fe^{2+} (upper plane) and Fe^{3+} (lower plane) aqueous solutions.

In the previous work, the presence of the Jahn-Tellller distortion in the first hydrated shell of the Fe^{2+} aqueous solution was questioned [8–10]. Jarzecki et al. pointed out that an Fe^{2+} cation was characterized by 6 electrons in the 5d orbits in a high spin state. In these 5 orbits, the d_π level was occupied by two electrons leading to a reduction of the electronic symmetry to form the Jahn-Teller effect. On the contrary, for the Fe^{3+} cation, whose d^5 electron configuration was characterized by a spherical symmetry, the Jahn-Teller effect disappeared [10]. However, these calculations contained only Fe^{2+} $(H_2O)_6$ clusters without any further water molecules and neglected important contributions such as the structural disorder effect that exists in real aqueous solutions, as well as their dynamic properties. In Tawun's work, which was based on the QM/MM simulation, the Jahn-Teller distortion in the Fe^{2+} aqueous solution could be found [9]. On the other hand, all the previous work was only theoretical and lacked some experimental evidence. Therefore, the combination of some theoretical (such as MD) and experimental (such as XAS) methods would provide a reliable description about the hydrated shells around metal ions

in aqueous solution.

The angular distribution function of the first hydrated shell is shown in Fig. 2, where the angle ψ is defined as the O-Fe-O angle. It can be seen that the angular distribution of Fe^{2+} and Fe^{3+} aqueous solutions is similar. However, a more concentrated distribution can be seen in the Fe^{3+} aqueous solution, which is consistent with a previous investigation showing that the Fe^{3+} cation has a more stable first hydrated shell. Both angular distributions have intense peaks when $1-\cos(\psi)$ equals 1 and 2, corresponding to ψ angles of 90° and 180°. Combined with the distribution functions, we can conclude that the first hydrated shell of both Fe^{2+}/Fe^{3+} aqueous solutions arrange as a regular octahedron. On the other hand, seven and eight coordinated species have been also observed in the MD simulations of Fe^{3+} aqueous solution, but they only account for about 0.5% and can be ignored in the following discussion. Their angular distribution functions are shown in Fig. 3 and their broadened peaks also indicate that two species are unstable.

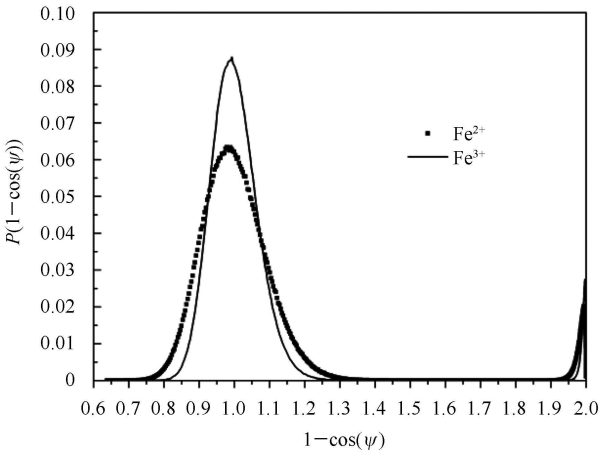

Fig. 2. The angular distribution function of the first hydrated shell for Fe^{2+} and Fe^{3+} aqueous solutions.

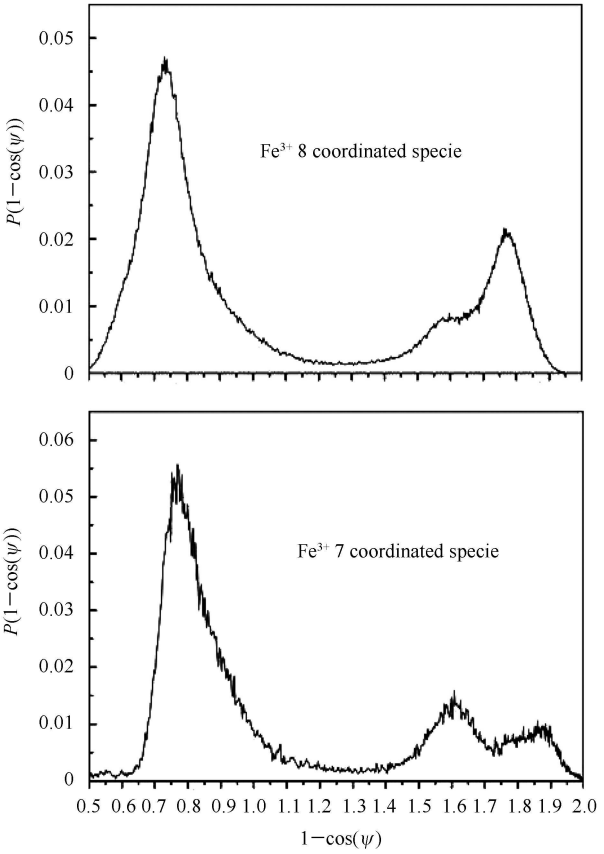

Fig. 3. The angular distribution function for 8- and 7-coordinated species in Fe^{3+} aqueous solution.

3.2 The XANES simulation

The experimental XANES for Fe^{2+} and Fe^{3+} aqueous solutions are shown in Fig. 4. It can be seen that Fe^{2+} and Fe^{3+} XANES have similar pre-edge peaks which are assigned to $1s$-$3d$ transition. The multiple scattering

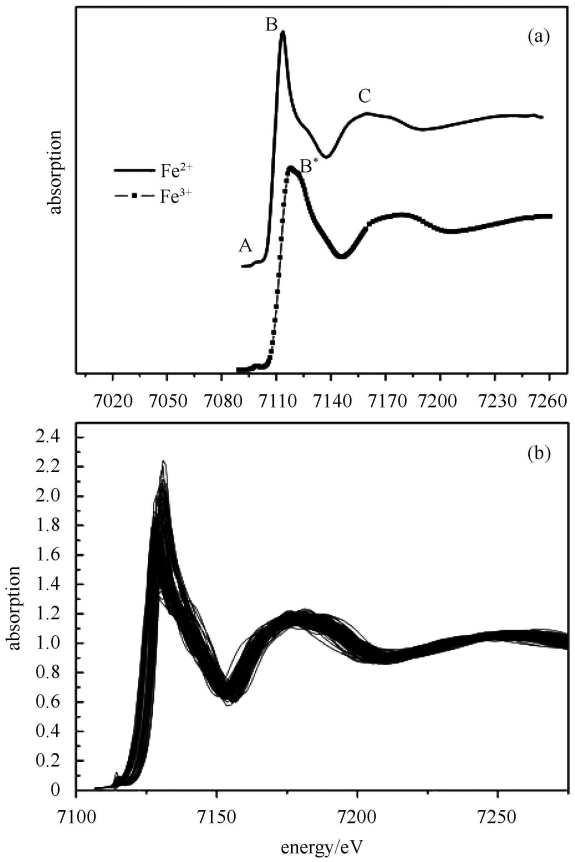

Fig. 4. The experimental XANES for Fe^{2+} and Fe^{3+} aqueous solutions (upper plane) and the calculated XANES spectra obtained from the instantaneous configurations given by the MD simulations (lower plane).

peak C in Fe^{3+} XANES moves to higher energy, indicating a longer Fe-O bond length than that in the Fe^{2+} aqueous solution. The main difference between an Fe^{2+} and Fe^{3+} XANES is the occurrence of the shoulder B' in the Fe^{3+} XANES.

The XANES is very sensitive to the local structure around an absorption atom. For the aqueous solution system, some previous investigations have proved that the structural disorder has a non-negligible influence on the XANES spectrum [23]. Therefore, a single structure obtained from instantaneous configurations in the MD simulation is not representative for all those structures in aqueous solution. We compare several calculated spectra obtained from the instantaneous configurations given by the MD simulations (Fig. 4(b)) and the structural disorder effect can be seen clearly, so a sum and average are necessary for the reproduction of metal cations in an aqueous solution. In order to quantitatively include the structural disorder effect in our XANES calculations, we carried out several XANES calculations from instantaneous configurations obtained from an MD trajectory. The configuration also includes the second hydrated shell since a previous investigation pointed out that the second hydrated shell contributes to the XANES [24]. In order to determine the minimum amount of sampled configurations necessary to be statistically significant, we calculated a residual function of each averaged spectrum, which is defined as follows:

$$\mathrm{RMS}(n)=\sqrt{\sum_i[\alpha^n(E_i)-\alpha^{n-1}(E_i)]^2}, \qquad (3)$$

$a^n(E_i)$ is the theoretical spectrum averaged over n configurations and the sum goes over all calculated energy points. The value of the RMS decreases down to $<1\times10^{-4}$ when n exceeds 150. Therefore, we calculate the spectra of both Fe^{2+} and Fe^{3+} aqueous solutions, which are summed and averaged over 150 "instantaneous spectra", and compare them with the experimental data (Fig. 5). It can be seen that the calculation reproduces the experimental spectra well, including pre-edge features, white lines, and post-edge broadened features. All these factors imply that the structures obtained from MD are credible. However, it is clear that the calculated spectra of both Fe^{2+} and Fe^{3+} aqueous solutions present more intense features than the corresponding experimental data in 7145–7200 eV, which is explained as the existence of 1s-3s multi-electrons excitations in this energy range [25] and this factor has not been considered in our theoretical calculation.

On the other hand, it is worth noting that the calculation of the same non-structural parameters used as Fe^{2+} will only move feature C of the Fe^{3+} aqueous solution to higher energy and feature B' will not appear, as shown in Fig. 5(b). In the XANES calculation program FEFF8.7, the charge transfer parameter ION can be used to adjust the charge transfer of Fe^{2+} and Fe^{3+}; it is worth noting that feature B' appears when the charge of the absorbing atom in Fe^{3+} is more transferred to O atoms (Fig. 5(c)). Therefore, feature B' can be assigned to the contribution of the charge transfer.

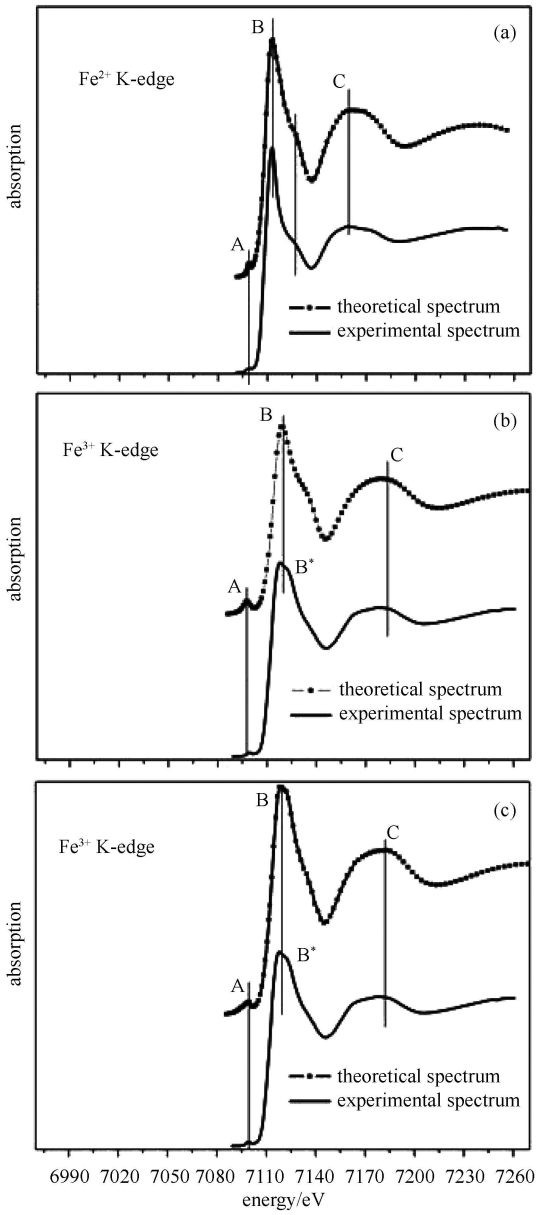

Fig. 5. The calculated and experimental spectra for Fe^{2+} aqueous solution (upper plane), Fe^{3+} aqueous solution with less charge transfer (middle plane), and Fe^{3+} aqueous solution with more charge transfer (lower plane).

4 Conclusion

This work demonstrates that the combination of MD simulations and XAS spectroscopy may provide a new and accurate structural tool to describe the local geometry of disordered systems such as aqueous solutions. Indeed, this layout is a powerful and reliable method for a quantitative consideration of structural disorder effect in XANES analyses.

We use this method to investigate the structure of Fe^{2+} and Fe^{3+} in aqueous solutions. The first hydrated shell of both aqueous solutions are characterized by a regular octahedron with a 2.08Å Fe-O distance for Fe^{2+} and 1.96Å for Fe^{3+}. The result supports Tawun's point that no Jahn-Tellller effect will exist in an Fe^{2+} aqueous solution. On the other hand, feature B', which is located at energy 1eV higher than WL in Fe^{3+} aqueous solution, may be assigned to the contribution of the charge transfer.

References

1 Weare H. Rev. Mineral, 1987, **17**: 143
2 Hochella F, Lower K, Maurice A et al. Science, 2008, **319**: 1631
3 Kerisit S, Cooke J, Spagnoli D et al. J. Mater. Chem., 2005, **15**: 1454
4 Spagnoli D, Cooke J, Kerisit S et al. J. Mater. Chem., 2006, **16**: 1997
5 Valiev M, Kawai R, Adams A et al. J. Am. Chem. Soc., 2003, **125**: 9926
6 Valiev M, YANG J, Adams A et al. J. Phys. Chem. B, 2007, **111**: 13455
7 Clark L, Hobart E, Neu P. Chem. Rev., 1995, **95**: 25
8 Franca F, Maurizio P, Alessandro T et al. Chemical Physics Letters, 1992, **199**: 518
9 Tawun R, Bernd R. J. Phys. Chem. A, 2003, **107**: 2324
10 Jarzecki A, Anbar D, Spiro G. J. Phys. Chem. A, 2004, **108:** 2726
11 Tomasi J, Persico M. Chem. Rev., 1994, **94**: 2027
12 Cossi M, Barone V, Cammi R. Chem. Phys. Lett., 1996, **255**: 327
13 McWeeny R, Dierksen G. J. Chem. Phys., 1968, **49**: 4852
14 Hay J, Wadt R. J. Chem. Phys., 1985, **82**: 270
15 Wadt R, Hay J. J. Chem. Phys., 1985, **82**: 284
16 Woon E et al. J. Chem. Phys., 1993, **98**: 1358
17 Kendall A et al. J. Chem. Phys., 1992, **96**: 6796
18 Giovanni C, Paola A, Nicolae P et al. J. Am. Chem. Soc., 2002, **124**: 1968
19 Berendsen C, Van D, Van R. Comput. Phys. Commun., 1995, **95**: 43
20 Darden T, York D, Pedersen L. J. Chem. Phys., 1993, **98**: 10089
21 Berendsen C, Postma M, Van F et al. J. Comput. Phys., 1984, **81**: 3684
22 Ankudinov L, Ravel B, Rehr J. Phys. Rev. B, 1998, **58**: 7565
23 Rehr J, Ankudinov L. Coord. Chem., 2005, **249**: 131
24 Joly Y. Phys. Rev. B, 1996, **53**: 13029
25 Paola A, Roscioni M, Chillemi G et al. J. Am. Chem. Soc., 2006, **128**: 1853